Calixarenes
Каликсарены

Макрогетероциклы
http://macroheterocycles.isuct.ru

Paper
Статья

# Self−Aggregation and Solubilizing Properties of the Supramolecular System Based on Azobenzenesulfonate Calix[4]arene and CTAB

Ruslan R. Kashapov,[a@] Alina M. Bekmukhametova,[a] Lucia Ya. Zakharova,[a]
Zaliya V. Akhmetzyanova,[b] Elena V. Popova,[a] Svetlana E. Solovieva,[a,b]
Igor S. Antipin,[a,b] and Alexander I. Konovalov[a]

[a]A.E. Arbuzov Institute of Organic and Physical Chemistry, Kazan Scientific Center, Russian Academy of Sciences, 420088 Kazan, Russian Federation
[b]Kazan Federal University, 420008 Kazan, Russian Federation
@Corresponding author E-mail: kashapov@iopc.ru

*The intermolecular interaction of azobenzenesulfonate calix[4]arene with cationic surfactant CTAB was studied by a complex of physicochemical methods. The influence of calix[4]arene:CTAB ratio on the form of the aggregates in their mixed composition in the aqueous medium was determined. Single-layer vesicles are formed in the equimolar azobenzenesulfonate calix[4]arene-CTAB mixture. A threefold increase in the proportion of CTAB leads to the enlargement of vesicles, namely, an increase in numbers of bilayers. Spectrophotometry was used to select the conditions for binding of the hydrophobic spectral probe Sudan I by this mixed composition. The fluorescence spectroscopy establishes dependence between the amount of encapsulated Rhodamine B and the size of the vesicle. Thus, the azobenzenesulfonate calix[4]arene–CTAB system is capable for binding of both hydrophobic and hydrophilic substrates depending on the components ratio.*

**Keywords**: Calixarene, surfactant, Sudan I, Rodamine B, solubilization, aggregation.

# Самоагрегация и солюбилизирущие свойства супрамолекулярной системы на основе азобензосульфонатного каликс[4]арена и ЦТАБ

Р. Р. Кашапов,[a@] А. М. Бекмухаметова,[a] Л. Я. Захарова,[a] З. В. Ахметзянова,[b]
Е. В. Попова,[a] С. Е. Соловьева,[a,b] И. С. Антипин,[a,b] А. И. Коновалов[a]

[a]Институт органической и физической химии им. А.Е. Арбузова Казанского научного центра РАН, 420088 Казань, Россия
[b]Казанский федеральный университет, 420008 Казань, Россия
@E-mail: kashapov@iopc.ru

*Комплексом физико-химических методов изучено межмолекулярное взаимодействие азобензосульфонатного каликс[4]арена с катионным ПАВ ЦТАБ. Установлено влияние соотношения каликс[4]арен:ПАВ на форму агрегатов смешанной композиции в водной среде. В эквимолярной смеси азобензосульфонатный каликс[4]арен-ЦТАБ формируются однослойные везикулы. Увеличение доли ЦТАБ до трехкратного избытка приводит к укрупнению везикул, а именно к увеличению количества бислоев. Спектрофотометрическим методом осуществлен подбор условий для связывания гидрофобного спектрального зонда Судан I в данной смешанной композиции. Методом флуоресценции установлена зависимость между количеством закапсулированного Родамина В и размером везикулы. Таким образом, система азобензосульфонатный каликс[4]арен–ЦТАБ способна к связыванию как гидрофобных, так и гидрофильных субстратов в зависимости от соотношения компонентов.*

**Ключевые слова**: Каликсарен, ПАВ, Судан I, Родамин В, солюбилизация, агрегация.

## Introduction

Supramolecular systems based on amphiphilic compounds refer to the most effective drug delivery systems.[1] Their main advantages are associated with nanoscale dimensions, low aggregation threshold, simple synthesis and ability to control the process of self-organization and the binding/release of guests. The literature describes an approach based on the combination of several components of a diverse structure due to various non-covalent interactions, *e.g.* hydrogen bonds,[2] metal-ligand coordination,[3] electrostatic, [4-6] pi-stacking,[7] and "host-guest" interactions[8] with the formation of superamphiphiles, which allowed creating a large number of systems possessing the properties of nanocontainers[9] and molecular devices.[10]

Due to the dynamic nature of the non-covalent interactions of the superamphiphiles, it becomes possible to easily control their self-assembly and the properties of the emerging structures under the influence of various external factors. A large number of examples of using the superamphiphiles has been demonstrated in the field of vesicles with controlled properties,[11] in particular, vesicles, the stability of which is controlled by the p*H*.[12] Moreover, the creation of superamphiphiles allows solving important practical problems related to a reduction of critical aggregation concentrations and toxicity, as well as an increase of affinity for guest molecules.

The use of calixarenes and surfactants[13,14,16-22] in the creation of superamphiphiles is of particular interest. It is known that macrocycles, thanks to the presence of a molecular cavity and the preorganization of functional groups, are able to participate in guest-host interactions.[16,17] Surfactants, in turn, have ability to form micellar aggregates with a hydrocarbon core, which can solubilize different hydrophobic substrates. On the other hand, interest in macrocycles is due to the specific geometry of their molecules, which is important in the design of drug delivery systems and the development of antiviral drugs.[18-20] In the process of formation of mixed surfactant–calixarene compositions one can observe: (1) the increase in the solubility of macrocyclic compounds;[23] (2) the activation of binding processes of hydrophobic and hydrophilic substrates by monitoring the morphology of mixed aggregates;[13-15] (3) the decrease in the critical aggregation concentration.[13] The non-toxicity of calixarenes and surfactants makes them attractive for constructing receptors and carriers in solving biotechnological problems.

In the present paper superamphiphilic systems based on azobenzenesulfonate calix[4]arene (ABSC) and cationic surfactant CTAB were designed. This work will focus on the following aspects: (1) the study of the influence of surfactants on the form of supramolecular aggregates of ABSC-CTAB; (2) study of the properties of the mixed ABSC-CTAB system as a nanocontainer for hydrophobic (Sudan I) and hydrophilic (Rhodamine B) substrates (Scheme 1).
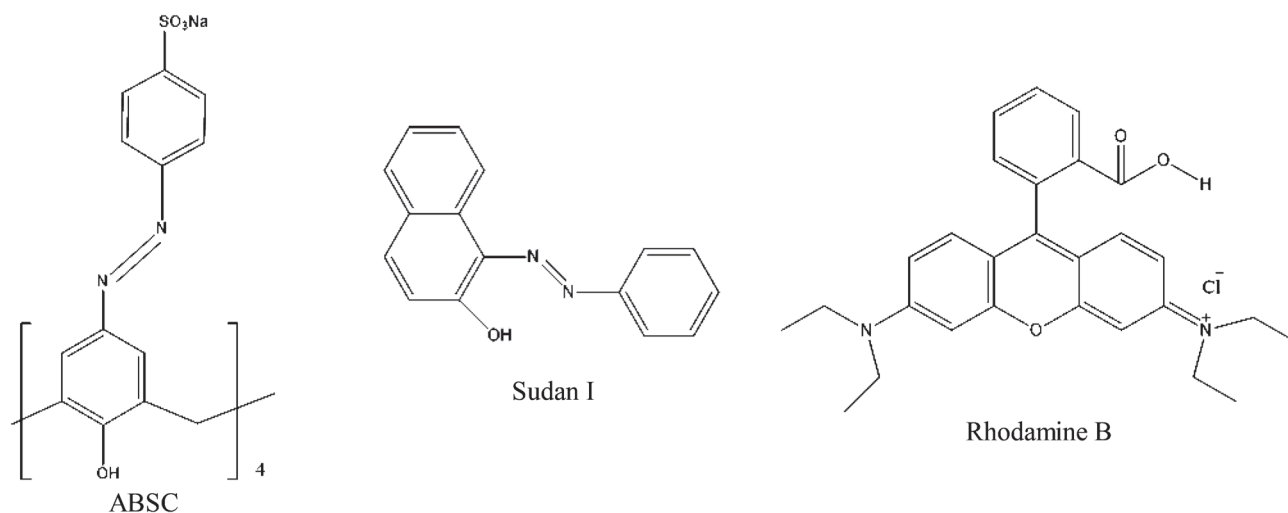
## Experimental

### *Materials*

Synthesis of *para*-(sulfophenylazo)calix[4]arene was carried out based by a published method[24] with modification of yielding. Briefly, the reaction mixture was evacuated, then 30 mL of water was added, and the mixture was dialyzed (1L×3). The dialyzed aqueous solution of the reaction product was treated with 50 % NaOH solution to p*H* 9-10 and stirred for an hour. The resulting reaction mixture was again dialyzed (1L×3) to p*H* 7. The residue was evaporated in vacuum. Yield: 1.52 g (92.7 %). MALDI-TOF *m/z*: 1183.2 [M–H$^+$+Na$^+$]. $^1$H NMR (600 MHz, 298 K, CD$_3$OD) $\delta_H$ ppm: 4.85 (s, 8H), 7.80 (s, 8H), 7.83 (d, 8H, *J*=8.7 Hz), 7.91 (d, 8H, *J*=8.7 Hz).

CTAB (Sigma-Aldrich, 98 %), rhodamine B (Acros Organics, ≥98%), 1-phenylazo-2-naphthol (Sudan I, Acros Organics) were used as received. Purified water (18.2 MΩ·cm resistivity) from Direct-Q 5 UV equipment was used for all solution preparations.

### *Methods*

The absorption spectra were recorded on a Specord 250 Plus spectrophotometer (Analytic Jena, Germany) using 1 mm path-length quartz cell. To investigate the solubilization of hydrophobic Sudan I, its solid sample was added into all solutions studied.



**Scheme 1.** Molecular structures of ABSC, Sudan I and Rhodamine B.

NMR spectroscopy experiments were performed on an Avance-600 (Bruker, Germany) spectrometer equipped with a pulsed gradient unit capable of producing magnetic field pulse gradients in the $z$ direction of about 56 G·cm⁻¹.

The diameters of the aggregates were determined by dynamic light scattering on a Zetasizer Nano instrument (Malvern Instruments, UK). The source of the laser radiation was a He-Ne gas laser with a power of 4 mW and a wavelength of 633 nm. For zeta potential measurement Zeta potential Nano-ZS (Malvern) with laser Doppler velocimetry and phase analysis light scattering was used. The temperature of the scattering cell was controlled at 25 °C. All light scattering data were processed using Malvern Zetasizer Software.

The fluorescence spectra were recorded on a Varian Cary Eclipse fluorescence spectrophotometer (USA) with the excited wavelength for Rhodamine B at 555 nm using 1 cm path length quartz cuvette. The emission spectra were recorded in the range of 560–750 nm. The Rhodamine B sample was added to ABSC-CTAB solutions with different concentrations of CTAB, so the final concentration of Rhodamine B in the solution was 25 mM. To separate the unloaded Rhodamine B from the one loaded in ABSC-CTAB vesicles Zeba Spin Desalting Column was used.

## Results and Discussion

The effective design of superamphiphilic systems is impossible without a detailed study of their structure. Therefore, on the first stage the mixed system based on ABSC and CTAB and the influence of the system components ratio on its morphology and properties were studied using spectrophotometry. The UV spectrum of ABSC in the aqueous medium is characterized by the presence of two absorption bands with maxima at 260 nm and 360 nm due to electronic transitions in the benzene and azobenzene rings, respectively (Figure 1). The addition of a threefold excess of CTAB relatively the macrocycle leads to a decrease in the intensity of the absorption band of ABSC at 360 nm and the appearance of a small arm at 460 nm, which is probably due to small conformational changes in the azobenzene ABSC groups in the presence of a surfactant molecule. A decrease in the intensity of ABSC absorption in the presence of CTAB can also be caused by formation of their mixed aggregates. It is interesting that a further increase of the surfactant concentration in comparison with macrocycle concentration causes a reverse increase in the intensity of the absorption band at 360 nm and its bathochromic shift by 8 nm (Figure 2).
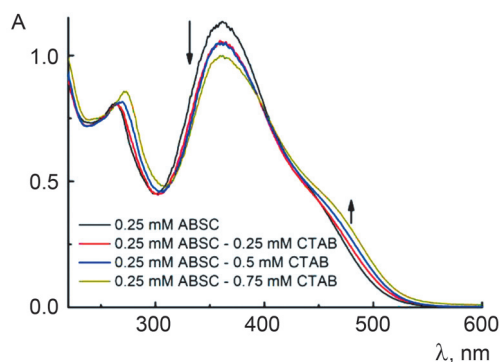


**Figure 1.** Absorption spectra of ABSC in aqueous solution at varying CTAB concentration from 0 to 0.75 mM (1 mm, 25 °C).

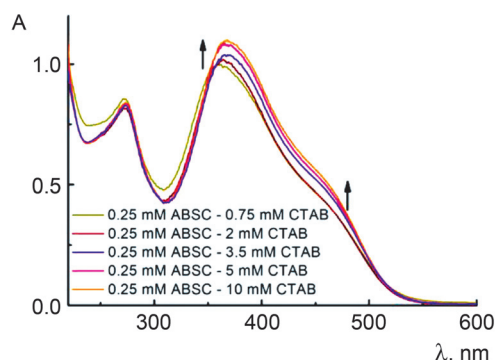This phenomenon is probably associated with morphological rearrangement of mixed aggregates.



**Figure 2.** Absorption spectra of ABSC in aqueous solution at varying CTAB concentration from 0.75 to 10 mM (1 mm, 25 °C).

On the spectra shown in Figures 1 and 2, there is another trend of ABSC absorption intensity depending on the surfactant concentration. Regarding to that, the dependence of the peak intensity ratio at 360 and 480 nm for the ABSC-CTAB system on the concentration of CTAB was constructed (Figure 3). The graph shows that in the range of CTAB concentrations up to 0.75 mM, the ratio of the ABSC absorption intensity decreases, and after this concentration the dependence goes to the plateau. It follows that the addition of CTAB molecules to the aqueous solution of ABSC results in the formation of mixed aggregates, the shape of which depends on the surfactant concentration. To verify this, at the next stage of the work the method of dynamic and electrophoretic light scattering was involved.
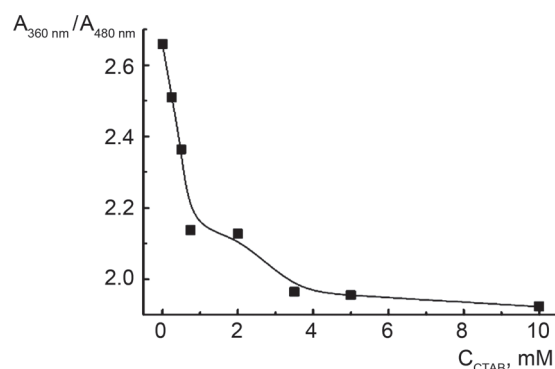


**Figure 3.** Dependence of the ratio of absorbance intensities of the peaks at 360 and 480 nm in aqueous solutions of ABSC-CTAB on the CTAB concentration.

Measuring the hydrodynamic diameters of joint aggregates in aqueous solutions of ABSC-CTAB, it was found that the initial increase in the proportion of surfactants leads to a significant increase in size of aggregates (Figure 4). For an equimolar solution of ABSC and CTAB, the formation of spherical particles about 10 nm in size was observed. Taking into account the size of the structural fragments of ABSC and CTAB, it can be assumed that

in the equimolar mixture these two components interact with each other to form single-layer vesicles. A threefold increase in the concentration of CTAB induces an increase in the hydrodynamic diameter to 56 nm, which also probably corresponds to aggregates of the vesicular structure, but with a large number of bilayers. When one molecule of ABSC interacts with three molecules of CTAB, a superamphiphilic complex with a large hydrophobic part is formed, which initiates the formation of aggregates with less surface curvature. A further increase of the surfactant concentration is accompanied by a decrease in the size of the vesicles, and at the CTAB concentration of 7.5 mM the diameter of the aggregates is 3.5 nm, which is characteristic of micelle-like structures. It is interesting to note that for the solution with a threefold excess of CTAB a negative value of the zeta potential (-49.0 mV) is observed, and the presence of 2 mM CTAB results in the recharging of the mixed ABSC-CTAB aggregates: the zeta potential of the aqueous solution of 0.25 mM ABSC-2 mM CTAB system equals to +53.2 mV. Thus, generalizing the results obtained by spectrophotometry, dynamic and electrophoretic light spectroscopy, it can be concluded that in the aqueous medium the molecules of ABSC and CTAB form spherical aggregates whose morphology depends on the surfactant concentration. The addition of threefold excess of CTAB causes the formation of vesicular-type aggregates, and the further addition of surfactant initiates the formation of micelle-like structures.
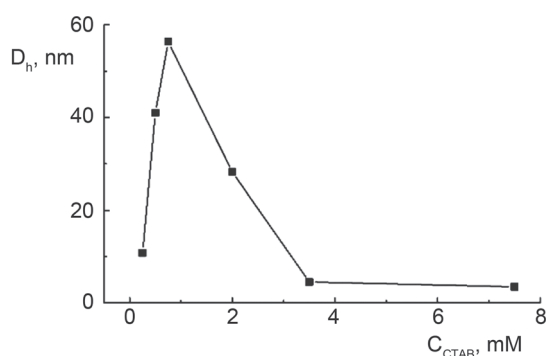


**Figure 5.** $^1$H NMR spectra of individual ABSC (a) and mixed ABSC-CTAB (b,c) solutions.



**Figure 4.** Dependence of the hydrodynamic diameter of ABSC-CTAB aggregates in aqueous solutions on the CTAB concentration, 25 °C.

Since ABSC and CTAB form supramolecular aggregates, it became important to know the nature of the interaction between these compounds by means of $^1$H NMR spectroscopy. Figure 5 shows $^1$H NMR spectra of ABSC alone and mixed with 10 and 30 mM CTAB, respectively. We see that the interaction of CTAB with a macrocycle results in a significant downfield shift of the ABSC aromatic proton signals, indicating the inclusion of surfactant in the aromatic cavity of the macrocycle. The formation of such kind of inclusion complexes is usually associated with the interaction of the calix[4]arene aromatic cavity and the charged head group of the surfactant cation. The increase of CTAB amount in comparison with the macrocycle is accompanied by a further descreening of the ABSC aromatic protons (by
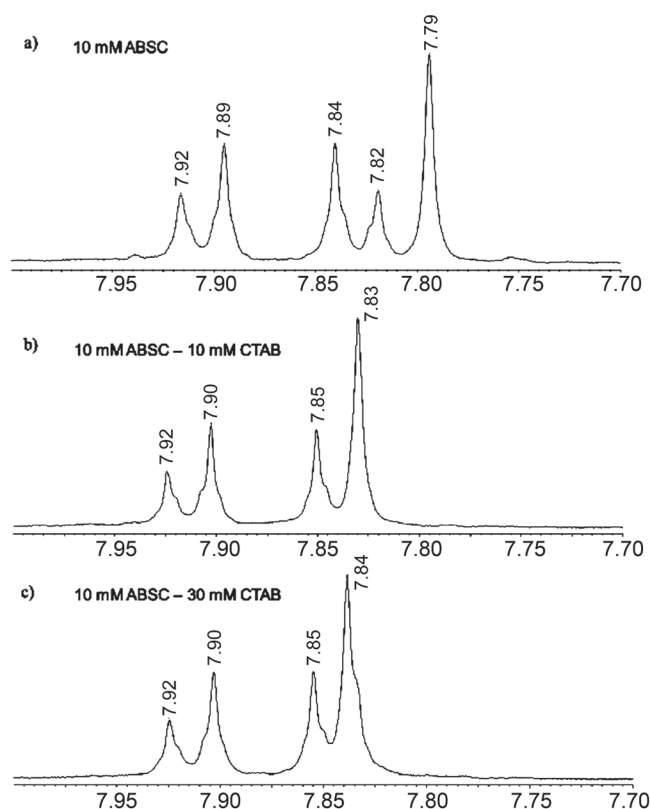
0.01 ppm), indicating that three CTAB ions can bind with the ABSC cavity.

At the next stage, the ABSC-CTAB system was tested as a nanocontainer for the model hydrophobic substrate Sudan I. This dye has a characteristic absorption band at 495 nm. The dependence shown in Figure 6 demonstrates that with increasing concentration of CTAB a gradual increase in the absorption intensity occurs, indicating the formation of aggregates with a hydrophobic core, which is capable of dissolving the hydrophobic probe. For the mixed ABSC-CTAB system, the absorption intensity of Sudan I also increases with the increase of surfactant concentration, but the solubilization capacity of the mixed ABSC-CTAB aggregates is lower than of the individual surfactant micelles.
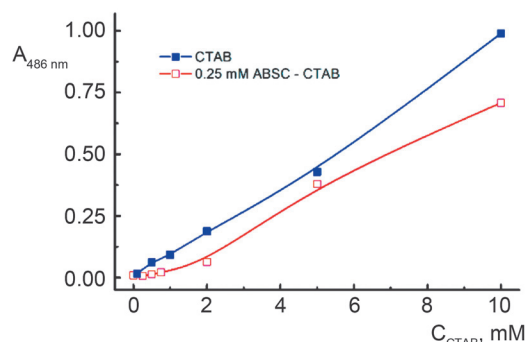


**Figure 6.** Intensity dependence of absorbance of Sudan I dye at 486 nm in aqueous solutions of CTAB in the absence and presence of 0.25 mM ABSC on the CTAB concentration (optical path 1 cm, 25 °C).
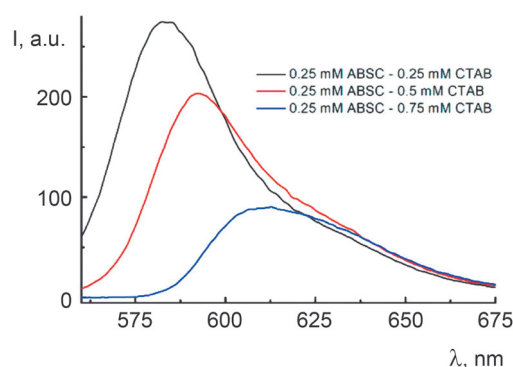
**Figure 7.** Changes in the fluorescence spectra of Rhodamine B in the ABSC-CTAB system at different concentrations of CTAB.



**Figure 8.** Schematic representation of Rhodamine B loaded into single-layer (a) and multilayer vesicles (b).

ABSC can act as a head group and promotes the formation of mixed micelles with a smaller hydrophobic core.

By a wide range of physicochemical methods we have demonstrated that the interaction of an equimolar amount of ABSC and CTAB results in the formation of single-bilayer vesicles. In addition, a threefold excess of CTAB towards ABSC leads to the formation of larger multilayer vesicles. It is known that vesicles serve as nanocapsules for the transport of hydrophilic drugs, therefore, at the next stage of the work, an evaluation of the loading of a hydrophilic component into the ABSC-CTAB vesicles became an interesting task. As a model hydrophilic substrate Rhodamine B, a fluorescent dye with a maximum absorption wave at 555 nm, was chosen. The evaluation of the Rhodamine B loaded into the vesicles core was carried out by fluorescence spectroscopy. From the fluorescence spectra, one can qualitatively judge about the amount of Rhodamine B, which is capable of penetrating through single-layer vesicles and through vesicles with a few numbers of layers (Figure 7). A decrease in the fluorescence intensity of Rhodamine B in the ABSC-CTAB system with increasing concentration of CTAB indicates that the amount of the fluorescent dye loaded into single-layer vesicles (0.25 mM ABSC: 0.25 mM CTAB) (Figure 8a) is greater than into multilayer vesicles (0.25 mM ABSC: 0.75 mM CTAB), which is due to the difficulty of Rhodamine B penetration through the several layers of vesicles (Figure 8b). Therefore, the composition of ABSC with CTAB could be used not only as the nanocontainer for hydrophobic drugs, but also as supramolecular nanocapsule for different hydrophilic therapeutic agents.

## Conclusions

By using a complex of physicochemical methods the intermolecular interaction of azobenzenesulfonate calix[4]arene with cationic surfactant CTAB was studied. The addition of CTAB molecules to the aqueous solution with ABSC molecules results in the formation of mixed aggregates, the shape of which depends on the surfactant concentration. With a ratio of ABSC:CTAB of 1:1, single-layer vesicles are formed, while a threefold increase in the proportion of CTAB towards ABSC causes the enlargement of the vesicles, namely, an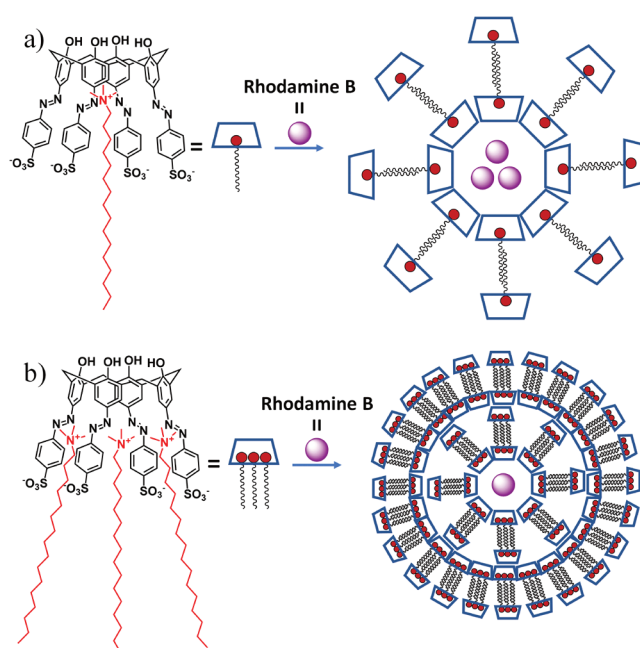 increase in the number of bilayers. A further increase in the CTAB concentration initiates the formation of mixed micelles, where ABSC acts as a head group. The ABSC-CTAB system was tested as a nanocontainer for the model hydrophobic substrate Sudan I. It was shown that the presence of ABSC in an aqueous solution of CTAB can promote the formation of mixed micelles with smaller hydrophobic core than that of individual CTAB micelles. In addition, the ABSC-CTAB system was studied as a nanocontainer for the model hydrophilic substrate Rhodamine B. The fluorescence method demonstrated the dependence between the amount of Rhodamine B loaded in the ABSC-CTAB vesicle and the size of this vesicle. Thus, the more layers in the vesicle, the lower the loading of the hydrophilic fluorescent dye. These experiments confirmed that the ABSC-CTAB system is capable of binding hydrophobic and hydrophilic substrates; this opens the perspective for the use of such superamphiphilic compositions as a nanocontainer for drug delivery.

## References

1. Schneider H.J. *Applications of Supramolecular Chemistry*. Boca Raton: CRC Press, **2012**. 453 p.

2.  Hermans T.M., Broeren M.A.C., Gomopoulos N., Smeijers A.F., Mezari B., Van Leeuwen E.N.M., Vos M.R.J., Magusin P.C.M.M., Hilbers P.A.J., Van Genderen M.H.P., Sommerdijk N.A.J.M., Fytas G., Meijer E.W. *J. Am. Chem. Soc.* **2007**, *129*, 15631–15638.
3.  Gohy J.F., Lohmeijer B.G.G., Varshney S.K., Schubert U.S. *Macromolecules* **2002**, *35*, 4560–4563.
4.  Kabanov A.V., Bronich T.K., Kabanov V.A., Yu K., Eisenberg A. *J. Am. Chem. Soc.* **1998**, *120*, 9941–9942.
5.  Han Y., Wang W., Tang Y., Zhang S., Li Z., Wang Y. *Langmuir* **2013**, *30*, 9316–9323.
6.  Kumar M., George S.J. *Chem. Asian J.* **2014**, *9*, 2427–2431.
7.  Zhang X., Chen Zh., Würthner F. *J. Am. Chem. Soc.* **2007**, *129*, 4886–4887.
8.  Bojinova T., Coppel Y., Lauth-de Viguerie N., Milius A., Rico-Lattes I., Lattes A. *Langmuir* **2003**, *19*, 5233–5239.
9.  Kim K.T., Meeuwissen S.A., Noltea R.J.M., van Hest J.C.M. *Nanoscale* **2010**, *2*, 844–858.
10. Wang Y., Ma N., Wang Zh., Zhang X. *Angew. Chem. Int. Ed.* **2007**, *46*, 2823–2826.
11. Zhang H., Sun L., Liu Zh., An W., Hao A., Xin F., Shen J. *Colloids Surf., A* **2010**, *358*, 115–121.
12. Sun T., Li Yu., Zhang H., Li J., Xin F., Kong L., Hao A. *Colloids Surf., A* **2011**, *375*, 87–96.
13. Kashapov R.R., Pashirova T.N., Kharlamov S.V., Ziganshina A.Yu., Zhiltsova E.P., Lukashenko S.S., Zakharova L.Ya., Latypov S.K., Konovalov A.I. *Phys. Chem. Chem. Phys.* **2011**, *13*, 15891–15898.
14. Kharlamov S.V., Kashapov R.R., Pashirova T.N., Zhiltsova E.P., Ziganshina A.Yu., Zakharova L.Ya., Latypov Sh.K., Konovalov A.I. *J. Phys. Chem. C* **2013**, *117*, 20280–20288.
15. Wang K., Guo D.S., Wang X., Liu Y. *ACS Nano* **2011**, *5*, 2880–2894.
16. Zakharova L.Ya., Konovalov A.I. *Colloid J.* **2012**, *74*, 194–206.
17. Francisco V., BasilioN., Garcia-Rio L., Leis J.R., Maques E.F., Vazquez-Vazquez C. *Chem. Commun.* **2010**, *46*, 6551–6553.
18. Basilio N., Martín-Pastor M., García-Río L. *Langmuir* **2012**, *28*, 6561−6568.
19. Zhiltsova E.P., Kashapov R.R., Zakharova L.Ya., Lukashenko S.S., Timosheva A.P., Kasymova E.M., Kayupov A.R., Burilov A.R. *Kinet. Catal.* **2012**, *53*, 231–238.
20. Kashapov R.R., Pashirova T.N., Zhiltsova E.P., Lukashenko S.S., Ziganshina A.Yu, Zakharova L.Ya. *Russ. J. Phys. Chem. A* **2012**, *86*, 200–204.
21. Gaynanova G.A., Bekmukhametova A.M., Sayfutdinova M.N., Gavrilova E.L., Zakharova L.Ya., Sinyashin O.G. *Russ. Chem. Bull.* **2015**, *8*, 1982–1985.
22. Gaynanova G.A., Bekmukhametova A.M., Kashapov R.R., Ziganshina A.Yu., Zakharova L.Ya. *Chem. Phys. Lett.* **2016**, *652*, 190–194.
23. Oshima T., Oishi K., Ohto K., Inoue K. *J. Inclusion Phenom. Macrocyclic Chem.* **2006**, *55*, 79–85.
24. Menon Sh.K., Patel R.V., Panchal J.G. *J. Inclusion Phenom. Macrocyclic Chem.* **2010**, *67*, 73–79.